Key Performance Indicators for Elastic Optical Transponders and ROADMs: The Role of Flexibility

Adaranijo Peters, Emilio Hugues-Salas, Matthias Gunkel and Georgios Zervas

Abstract

Flexible optical networks will provide the required service diversity to manage unpredictable traffic patterns and growth. However, a key challenge is to quantify flexibility in order to indicate the associated performance of individual components and subsystems required to support networks and correlate it with other figures of merit. Measurable key performance indicators will aid the process towards the design and deployment of cost effective and efficient optical networks. Moreover, the design and placement of network elements within a network influences the resultant network-wide flexibility and performance. In this paper, we highlight critical design parameters for key optical components, optical transmission and switching subsystems using flexibility as an additional figure of merit. We derive models to measure the flexibility of key optical components, optical transmission and switching subsystems based on entropy maximization. Using these models, we evaluate flexibility and design trade-offs of the presented enabling technologies with other key performance indicators such as spectral efficiency, lightpath reach, total capacity, normalized cost, connectivity and others. This study provides an advanced and more informed set of design rules that quantify and visualize the different degrees of flexibility of enabling technologies and associated performance based on required specification and/or functionality.

Key words

Key performance indicators; Flexibility; Wavelength selective switch; Spectrum selective switch; Bandwidth variable transponder.

1. INTRODUCTION

Over the past few years there has been a rapid increase in the growth of global IP traffic attributed to increased consumer demands for bandwidth hungry services such as cloud computing, online gaming and high definition video [1]. Elastic optical networks (EONs) offers a promising solution to meet the demand of exponential growth and unpredictability of internet traffic patterns. EONs supports spectrum utilization in a flexible manner and the transmission of variable bandwidth optical paths with optimized transmission reach [2, 3]. Also, the benefits of EONs have been investigated in [4-7] showing the potential improvements in cost, required spectral occupancy and energy efficiency. Based on the aforementioned EON features, optical networks equipped with flexibility and resilience must be designed and deployed in a cost-efficient manner. Network elements such as; opto-electronic and optical components, optical subsystems, optical nodes and network topologies determines the resultant flexibility and performance of the entire network. In more detail, each element is an important building block of the network, therefore different design configurations and architectures as well as placement of these elements across the network determines its overall flexibility and performance. One potential technique to accurately equip optical networks with flexibility and efficiency involves the design of optical networks using flexibility as a figure of merit [8]. Therefore quantitative flexibility measurement and its correlation to other key performance indicators (KPIs) could allow operators to design networks with different levels of flexibility while achieving the necessary transmission and network performance and in turn deliver efficiency in design and network operations.

As an important building block of flexible optical networks, reconfigurable optical add/drop multiplexers (ROADMs) enable network operators to dynamically route and switch wavelength channels through software control resources without the exact knowledge of traffic growth patterns [9]. Several ROADM designs are implemented using specific optical components such as: wavelength selective switches (WSSs), spectrum selective switches (SSSs), multicast switches (MCSs) and different transponder configurations. However, the selection and combination of these components are based on the flexibility and performance requirements. Furthermore, ROADM architectures equipped with colourless, directionless and contentionless (CDC) capabilities further increase the flexibility, functionality and reconfigurability of optical node operations [9-14].

In our previous studies [15, 16], models to measure the flexibility of an $N \times M$ WSS/SSS design without contention and multi-carrier bandwidth variable transponders (BVTs) with optical carrier contention were presented. Using these models, design trade-offs between different port dimensions of WSS and SSS were analyzed. Furthermore, the flexibility of the different BVT configurations were compared and associated with KPIs which include capacity, connectivity, granularity and spectral efficiency. Finally, individual components were combined to form subsystems for add/drop networks. The flexibility models of the optical subsystems were presented and a comparison of performance trade-offs of the different subsystems were analyzed considering different figures of merits. This paper delivers a more comprehensive and an all-round analysis of an extensive range of key opto-electronic and optical components and optical subsystems following the preliminary study and results reported in [15, 16]. An extensive range of WSS/SSS designs including an $N \times M$ WSS/SSS without wavelength contention, an $N \times M$ WSS/SSS with wavelength contention and an $N \times M$ WSS/SSS with input-output (I/O) port dimension reconfigurability are considered. The derivation of the flexibility models of each WSS/SSS design are presented and explained. In addition, theoretical results and analysis of

WSSs/SSSs designs are presented which highlight important design parameters to be considered for different performance requirements and network functions. Furthermore, the models to measure the flexibility of multi-carrier BVTs with and without optical carrier contention are presented and explained. KPIs including lightpath reach, cost, through loss, capacity, connectivity, spectral efficiency, flexibility and reconfigurable design features of different transponder configurations are evaluated and compared. Using theoretical analysis and results presented, we create design rules for BVTs with different performance requirements and analyze the relationship between KPIs and design parameters. Finally we describe and present models to measure the flexibility of subsystems for add/drop networks and evaluate the flexibility and design trade-off of these subsystem.

The rest of this paper is organized as follows: In section 2, a review of key enabling technologies with application in ROADMs design, add/drop networks and EONs are discussed. In section 3, we describe measurable KPIs for design of optical networks. Also, the schematic and potential benefits of an $N \times M$ WSS/SSS based ROADM is presented. Section 4 details models to measure the flexibility of $N \times M$ WSS/SSS under different design configurations. Furthermore, we highlight design rules and analysis for different performance requirements. Section 5 details models to measure the flexibility of a range of BVTs designs. The KPIs of different BVT configurations are measured and evaluated showing design dependency and trade-offs for different performance requirements. Section 6 details models to measure the flexibility of optical subsystems for add/drop networks and EONs. Furthermore, flexibility analysis and design trade-off of these optical subsystem are discussed. Section 7 presents the conclusion of the paper.

2. REVIEW ON ENABLING TECHNOLOGIES

The WSS is a key component for ROADM design because it allows dynamic routing and switching of wavelength channels from any input port to any output port. Additionally, WSSs are bidirectional and can perform blocking and power equalization of wavelength channels [17, 18]. The $1 \times M$ WSS has been demonstrated using numerous switching technologies including liquid crystal on silicon (LCOS) element [19] and micro electromechanical system (MEMS) mirrors [20]. Also, in [18] a performance analysis and summary of the different switching engine technologies has been presented. The $N \times M$ WSS can be designed by connecting an $N \times 1$ WSS with a $1 \times$ M WSS in series or N number of $1 \times M$ WSSs with M number of $N \times 1$ WSSs in parallel [9, 17]. However, these designs have drawbacks as wavelength contention is present in the former and the latter is not cost effective because a high number of $1 \times M$ and $N \times 1$ WSSs are required for high dimension switches. These drawbacks in cost and wavelength contention are mitigated with the design of an $N \times M$ WSS as single component without internal wavelength contention. Numerous studies have demonstrated the $N \times M$ WSS as a single component based on LCOS technologies [21, 22]. Additionally, the $N \times M$ WSS without contention offers potential benefits such as supporting multi-flow application [23] and the realization of CDC ROADM architecture [9]. Fixed grid WSS-based ROADMs are restricted to 50GHz or 100 GHz channel spacing, therefore cannot meet the requirement of the recommended ITU-T grid G.694.1 for EONs [24]. This drawback has been eliminated with the recent introduction and deployment of spectrum selective switches (SSSs) also known as bandwidth variable wavelength selective switches (BV-WSSs). The SSS provides finer spectrum switching granularity than the WSS and can dynamically switch and block spectral slots of different widths and sizes. Thus, optical paths with variable bandwidths and modulation formats can be efficiently managed. To this end, upgrading the WSS to the SSS allows for flexible-grid ROADMs [8, 25, 26].

Another important component that can be employed in ROADM structure is the multicast switch (MCS), which is also known as the transponder aggregator (TPA). The MCS is fabricated using planar lightwave circuit (PLC) technology and has been used to deliver the CDC capabilities in ROADMs architecture. The MCS is reliable, supports large scale production and is implemented using a compact multicast switch design composed of optical splitters and optical switches [27, 28]. However in terms of scalability, there is an increase in loss as the port count increases due to the presence of the optical splitters.

Flexible transponders are vital technologies required to meet the dynamic trends and exponential growth of internet traffic and deliver CDC ROADM capabilities by varying programmable/reconfigurable transmitter features such as modulation formats, symbol rates, tunable wavelength channels/spectral slots and number of carriers. The emergence of advanced digital signal processing (DSP) techniques and high performance digital to analogue converters (DAC) have given rise to software defined/adaptable transmitters. Such transmitters have been demonstrated in [29-31] where higher-order modulation formats and multiple data rates were achieved. The flexibility of the optical transmitter is further enhanced using multi-carrier technologies. Several studies have demonstrated multi-carrier solutions such as electrical and optical orthogonal frequency division multiplexing (OFDM) [32-34], Nyquist wavelength division multiplexing (N-WDM) [35] and optical arbitrary waveform generator (OAWG) [36]. Additionally in [2], the implementation of BVTs for EONs using various multi-carrier technologies has been discussed. The concept of sliceable bandwidth variable transponders (SBVTs) also called multiflow optical transponders has recently emerged as an innovative technology to improve flexibility and efficiency of network operations [2, 37]. Different combination of multiple optical paths with variable/equal bandwidth are formed and routed or sliced to the same or different destinations. Various architectures for SBVT designs have been proposed and demonstrated in [38-40]. Also a cost analysis of SBVT in a network scenario has been presented in [41], showing that SBVT reduce the cost of transponders by 30%.

3. KEY PERFORMANCE INDICATORS USED IN DESIGN OF OPTICAL NETWORKS

In this section, measurable KPIs for optical components and subsystems are discussed. In addition, we present a route and select ROADM which is implemented using a set of two $N \times M$ WSSs/SSSs and highlight the potential benefits in terms of flexibility and node scalability.

3.1 Measurable Key Performance Indicators

Measurable KPIs are vital for delivering cost-effective and efficient network design and operations. In this paper, the study focuses on the component and subsystem level design of the networking layer. Therefore the KPIs considered for component and subsystem design include capacity, spectral efficiency, cost, lightpath reach, through loss, connectivity and flexibility. Capacity (bits/s) is a measure of the amount of bits transmitted per second over an established transmission link. Spectral efficiency is a measure of spectrum utilization and is the ratio of transmitted bitrate to the required spectrum (b/s/Hz). Lightpath reach is a measure of the maximum distance a transmitted optical signal can reach without signal degradation. Connectivity is a measure of the number of successful links that can be established between network elements. Cost is the measure of the economic value of networks elements, which can be further be classified in terms of capital expenditure (CAPEX) and operational expenditure (OPEX). Through-loss (dB) is a measure of power loss of an optical signal when it is transmitted/passed through network elements. Each of the KPIs mentioned are important as standalone indicator in the design and deployment of optical networks. However in order to deliver cost efficient networks, it is important for network operators to understand the interrelation between each design parameter and KPIs. For example, cost is an important metric for deploying networks. However how does cost relate to connectivity or lightpath reach? Furthermore, what combination of network element design parameters are required in any given scenario to provide efficient optical networks or achieve certain functions? Another question is how much flexibility in the network is required to deliver a certain performance without overprovision of resources? Understanding the solution to such questions is key for efficient use of resources which may in turn lead to a reduction in cost, a reduction in component/network design complexity and a lower equipment manufacturing time.

Flexibility is the ability of a system to adapt to change and has been introduced as a KPI in [8]. In more detail, flexibility can be further defined in several contexts based on the functionality and design characteristics of the network element. For instance, a device which has the ability to reconfigure its structure to build different configurations or architectures has architectural flexibility, a device which has the ability to map channels from different inputs to different or the same output has routing flexibility, a device which has the ability to connect single/multiple input ports to single/multiple output ports in various ways and multiple dimensions (space and spectrum) has switching flexibility and a subsystem which has the ability to support several bitrates and functions (e.g., spectrum channel filtering and power equalization) has channel and functional flexibility. The flexibility of a system can be quantitatively measured considering the maximum entropy of system. The flexibility of a system is obtained by $F(S) = log(M)$ where $S = \{s_1 s_2 \ldots\ldots s_m\}$ is the set containing all the possible states of the system at any instant in time and M is the total number of different states assuming all states are equiprobable to achieve maximum entropy. The derivation of this flexibility measurement approach has been explained in detail in [8]. Also in [42], the flexibility measurement approach mentioned above has been utilized to measure and evaluate the flexibility of different add/drop structures considering the drop direction only. This measurement approach of flexibility can be used to measure the flexibility of single optical components with different functionalities, a combination of optical components, optical node architectures and optical network topologies. Table 1 shows the list and definition of all parameters used in the derivation of all flexibility models in this paper

TABLE 1
PARAMETER DEFINITIONS

Parameter	Definition
N	Number of input ports/number of BVTs in a subsystem
M	Number of output ports
P	Total number of ports
W	Number of wavelength channels/number of tunable wavelength channels
k	Spectral granularity factor
kW	Number of spectral slots number/number of tunable spectral slots
a	Number of single wavelength channel/spectral slots that can be to be passed from N input ports to M output ports at the same time
x	Maximum number of single wavelength channels/ spectral slots than can be passed from N to M output ports at a time
D	Total number of optical carriers
u	Number of optical carriers (optical channels) transmitted at the same time
B	Number of programmable modulations formats
E	Number of programmable symbol rates
s	Number of programmable electrical subcarriers
c	Number of BVTs transmitting at the same time / number of active input ports
i	Number of active input ports on the MCS that are unblocked

3.2 ROADM based on N × M WSS/SSS

Fig. 1(a) and 1(b) presents a schematic of a route and select ROADM implemented using two $N \times M$ WSSs and two $N \times M$ SSSs respectively. In Fig. 1(a), the fixed grid add/drop network consists of fixed bitrate single carrier transmitters/receivers where add/drop functions are performed. In Fig. 1(b), multi-carrier bit rate variable transmitters/receivers are present in the elastic add/drop network where add/drop functions of optical paths with variable spectral occupancy are performed. Unlike conventional route and select ROADMs implemented using two $1 \times M$ WSSs/SSSs for each node degree, two high port count contentionless $N \times M$ WSSs/SSSs are used instead. This design offers potential benefit of reduced cost, because the number of optical components ($N \times 1$ and $1 \times M$ WSSs/SSSs) required for node degree expansion are reduced and only two high port dimension $N \times M$ WSSs/SSSs can be used to provision for node degree expansion. Another potential benefit is improved internal routing flexibility as several internal paths between node degrees can be mapped out offering improved connectivity and additional paths for dynamic functionality such as signal regeneration and packet switching.

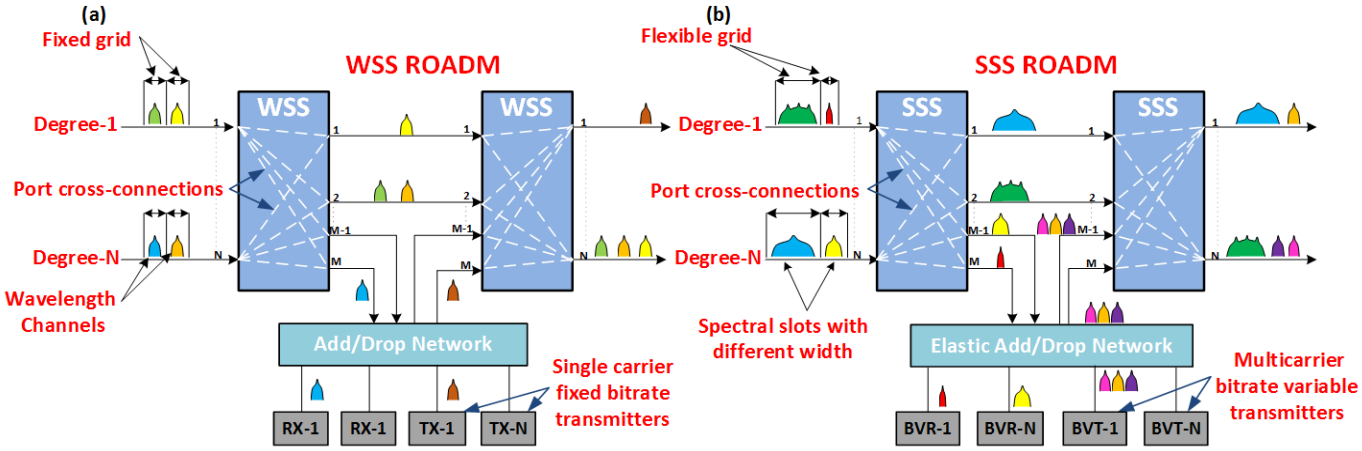

Fig. 1. Route and Select ROADM implemented using two $N \times M$ WSS/SSS.

4. Flexibility Measurement Analysis and Design Rules for $1 \times M$ and $N \times M$ WSS/SSS

In this section, we propose models to measure the flexibility of $N \times M$ WSS/SSS under different design conditions based on entropy maximization. Furthermore, we evaluate flexibility and trade-off of performance and design parameters.

4.1 Wavelength Selective Switch

1) *$N \times M$ WSS without wavelength contention*: An $N \times M$ WSS design without internal wavelength contention is considered. In this design, multiple copies of the same wavelength channel or multiple wavelength channels can be independently switched or blocked from any input port to any output port as long as wavelength conflicts are avoided i.e., switching copies of the same wavelength channel to the same output port. Therefore this device provides contentionless spectrum and space switching flexibility. Fig. 2 illustrates possible designs of an $N \times M$ WSS

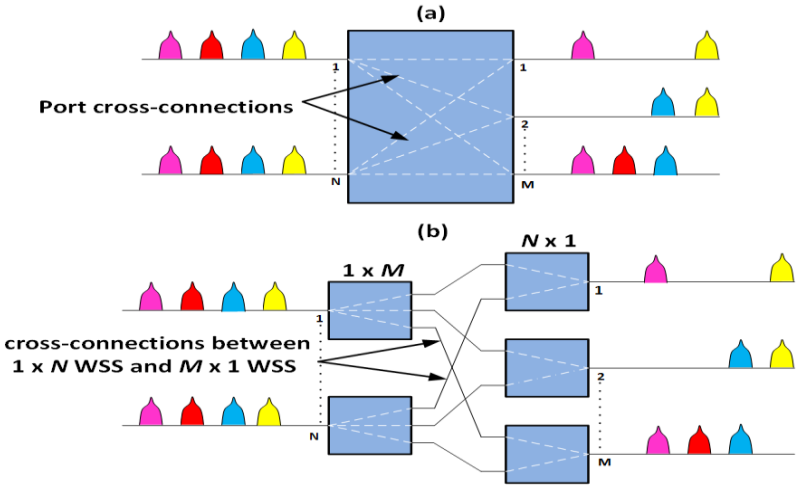

Fig. 2. Designs of $N \times M$ WSSs without wavelength contention.

without internal wavelength contention. Fig. 2(a) illustrates a design of a contentionless $N \times M$ WSS as a single component while in Fig. 2(b) illustrates a different design of a contentionless $N \times M$ WSS implemented by connecting N incoming $1 \times M$ to M outgoing $N \times 1$ WSSs in parallel (i.e., for an N x M port dimension N number of $1 \times M$ WSSs and M number of $N \times 1$ WSSs are required).

To measure the flexibility of the $N \times M$ WSS, we assume that the number of copies of the same wavelength channel that can be passed from $\boldsymbol{N}$ input ports to M output ports at the same time is a, thus the number of copies of a unique wavelength channel that are blocked is $(N - a)$ and x is the maximum number of copies the same wavelength channel that can be passed. Assuming the WSS supports W channels and a single or multiple wavelength channels can be switched or blocked across different cross-connections between N inputs and M output ports. The flexibility of the $N \times M$ WSS is

$$F(S) = W log\left(\sum_{a=0}^{x} \frac{M!}{(M-a)!}\binom{N}{N-a}\right) \qquad (1)$$
$$if\ N \leq M, x = N\ and\ if\ N > M, x = M$$

The proposed model in Eq. (1) can be applied to measure the flexibility of any port dimension of WSS. Fig. 3 shows the measured flexibility of a 20 port WSS design without contention with different port dimensions. The flexibility for each port dimension is measured across a different number of wavelength channels. The diagram shows that the flexibility is the highest for the 10×10 port dimension across all wavelength channels with 100 wavelength channels showing the highest flexibility. The diagram also shows that by decreasing the balance between $\boldsymbol{N}$ input and M output ports, the flexibility is reduced due to lower port cross-connections. Such analysis is therefore important for the design of $N \times M$ WSS as the port cross-connection and spectrum range are vital to the resultant flexibility and connectivity of the device.

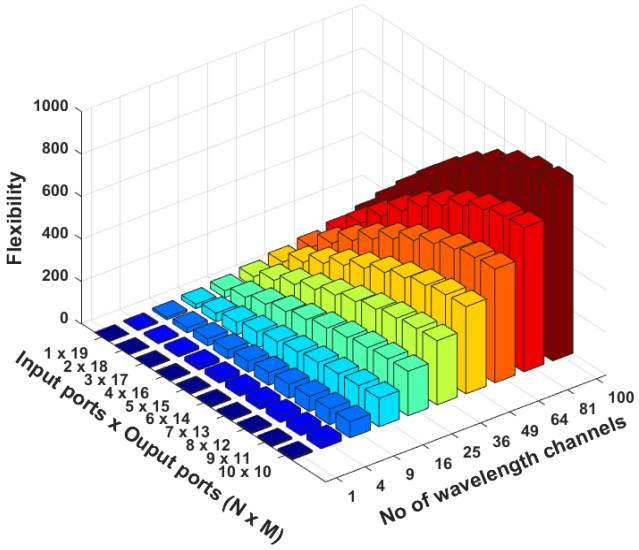

Fig. 3. Measure flexibility of different port dimensions of a WSS.

2) *$N \times M$ WSS with wavelength contention*: For this case, an $N \times M$ WSS design with internal wavelength contention is considered. The flexibility and connectivity of this WSS design is decreased as multiple copies of the same wavelength cannot be passed from multiple input ports to multiple output ports simultaneously (i.e., no wavelength re-use). An example of such an $N \times M$ WSS design is implemented by connecting $N \times 1$ WSS and $1 \times M$ WSS in series which is illustrated in Fig. 4.

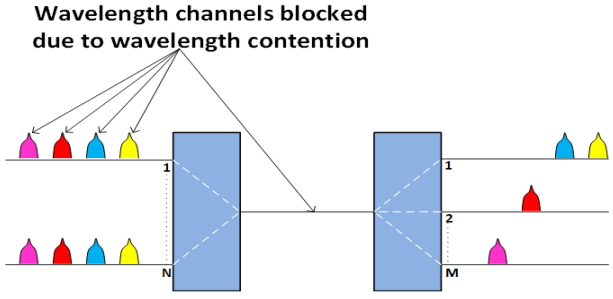

Fig. 4. Design of an $N \times M$ WSS with wavelength contention.

The model for measuring flexibility of this WSS design is derived in a similar way to the WSS design without internal contention. However the difference is that the maximum number of the same wavelength channel x that can be passed from N input ports to M output ports is one. Thus the flexibility is

$$F(S) = Wlog\left(\sum_{a=0}^{1}\frac{M!}{(M-a)!}\binom{N}{N-a}\right) \qquad (2)$$

A comparison of the measured flexibility of a 4 × 16 WSS design without internal wavelength contention and with internal wavelength contention is presented in Fig. 5. A WSS design with a 4 × 16 port configuration has been presented in [43] and experimentally demonstrated in a datacentre network scenario [44]. Fig. 5 shows that the difference in flexibility between the two 4 × 16 WSS designs increases as the number of wavelength channels increase with the contentionless WSS exhibiting the highest flexibility. This increase is due to the fact that the contentionless N × M WSS design allows multiple copies of the same wavelength channel to be successfully passed from N input ports to M output ports at the same time. While internal wavelength blocking is present in the $N \times M$ WSS design with internal wavelength contention and therefore less wavelength resources can be used. Thus, the contentionless $N \times M$ WSS provides greater flexibility and connectivity.

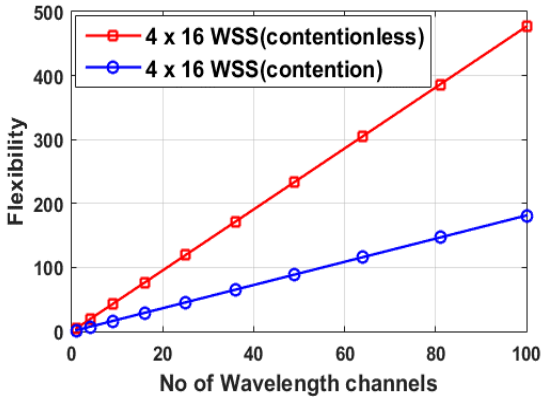

Fig. 5. Comparison of the flexibility of 4 × 16 WSS without contention and with contention.

3) *$N \times M$ WSS with input-output (I/O) port dimension reconfigurability*: A design of $N \times M$ WSS which supports (I/O) port dimension reconfigurability is considered i.e., the $N \times M$ WSS has the capability to rearrange its port dimensions/configurations based on the function or application required. Therefore, this device provides architectural flexibility, in addition to spectrum and space switching flexibility. Fig. 6 illustrates a 10 port WSS design with possible port reconfigurations which is reconfigured from a 2 × 8 port dimension to a 4 × 6 port dimension.

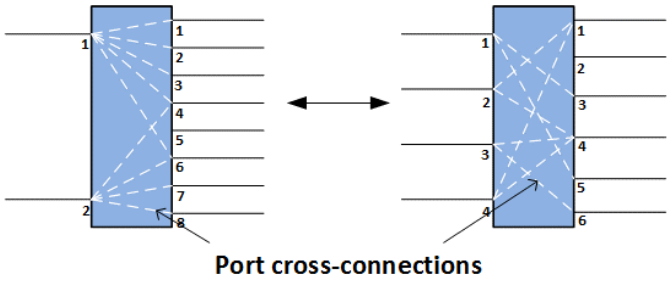

Fig. 6. $N \times M$ WSS with I/O port dimension reconfigurability.

To measure the flexibility, it is assumed that the total number of ports $P = (N + M)$ for all possible port dimensions. Thus for every value of N, $M = P - N$. Suppose a WSS without internal contention can be independently configured to different port dimensions while supporting W wavelength channels. The flexibility is

$$F(S) = log\left(\sum_{N=1,}^{(P-1)}\left(\left(\sum_{a=0}^{x}\frac{(P-N)!}{((P-N)-a)!}\binom{N}{N-a}\right)^{W}\right)\right) \qquad (3)$$
$$if\ N \le P-N, x = N\ and\ if\ N > P-N, x = P-N$$

Note that the flexibility of this WSS design with internal contention is modeled in a similar way, the only difference is the value of maximum

number of copies of the same wavelength channel x that are allowed to pass through is one. Fig. 7 shows a comparison of a non-configurable 1 × 19 WSS, a non-configurable 10 × 10 WSS and a 20 port WSSs with different step sizes of port reconfiguration granularity (step 1: 1 × 19⇔ 2 × 18 etc., step 2: 1 × 19⇔3 × 17 etc.). Note that the connectivity of each WSS design is defined as the total number of possible cross-connections between input and output ports i.e., connectivity is equal to input ports N multiplied by the output ports M. It is observed that the WSS with the most granular step of 1 has the highest flexibility, and hence flexibility decreases as the granular step size for port reconfigurability increases. On the other hand, it should be noted that the non-configurable 10 × 10 WSS offers a higher achievable connectivity than the reconfigurable 20 port WSSs with step sizes 2, 4 and 8. This is due to the fact that all possible port configurations of the listed step sizes have a lower number of port cross connections than the 10 × 10 WSS.

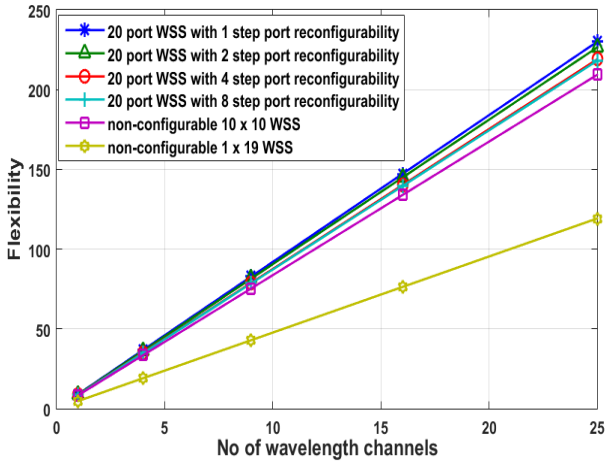

Fig. 7. Comparison of a non-configurable 1 × 19 WSS, 10 × 10 WSS and 20 port WSS of different steps of port reconfigurability.

4.2 Spectrum Selective Switch

1) *N × M SSS without internal contention*: An $N \times M$ SSS without internal contention is considered. In this design, a single or multiple spectral slots of different widths can be independently switched or blocked between N input and M output ports. This device provides contentionless space switching and finer spectral switching flexibility when compared to the WSS. Fig. 8 presents an illustration of an $N \times M$ SSS as a single component. It should be noted that this $N \times M$ SSS design can also be implemented by connecting N incoming $1 \times M$ SSSs and M outgoing $N \times 1$ SSSs in parallel. In flex-grid networks, a signal may occupy one or more spectral slots with infinite number of combinations of spectral slot sizes depending on the spectral granularity and requirements of the specific channel. For this study, due to complexity and dynamic nature of the flex-grid networks we consider a spectral granularity factor. i.e., assuming the channels of a fixed grid network have 50GHz channel spacing and the flexible grid network has 12.5GHz spectral slot spacing. In this scenario, we assume that there are 4 spectral slots in the flexible grid system for every wavelength channel in the fixed grid network. This approach for flexibility measurements of flex-grid systems was demonstrated in [8, 15, 16].

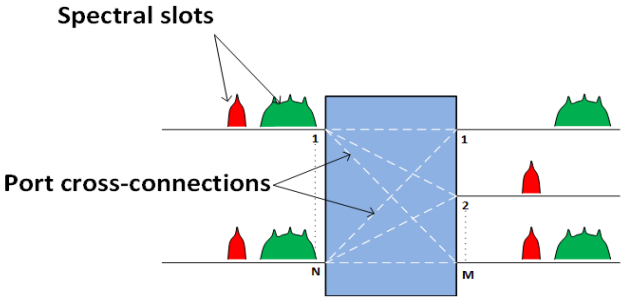

Fig. 8. Design of an N × M SSS without internal contention.

The model to obtain the flexibility is formulated in a similar way to the WSS without internal wavelength contention. Suppose the spectral granularity factor is k, hence kW spectral slots (over the same spectral range with the WSS) can be independently selected, switched or blocked from any N input port to any M output ports. The flexibility is

$$F(S) = kW log\left(\sum_{a=0}^{x} \frac{M!}{(M-a)!}\binom{N}{N-a}\right) \qquad (4)$$

$$if\ N \leq M, x = N\ and\ if\ N > M, x = M$$

Additionally, Eq. (4) can be applied to measure the flexibility of any dimension of the SSS. Fig. 9 illustrates the measured flexibility of contentionless WSS and SSS of various port dimensions across different number of wavelength channels. The flexibility of the SSS for all cases was calculated with a spectral granularity of 12.5GHz. It is observed that increasing the number of wavelength channels impacts the flexibility of the SSS more than the WSS for each pair of port dimensions, this is due to the finer spectrum switching granularity of the SSS. This effect is critically more impactful on high dimension switches. However, trade-offs between flexibility and port connectivity where observed as indicated in Fig. 9. For instance, the 5 × 6 SSS has greater flexibility than the 10 × 11 WSS but with a lower port connectivity. The same trade-off exists between the 2 × 3 SSS and the 5 × 6 WSS. Therefore, such results directly feed to a more informed design for a ROADM in terms of the different levels of flexibility and connectivity required.

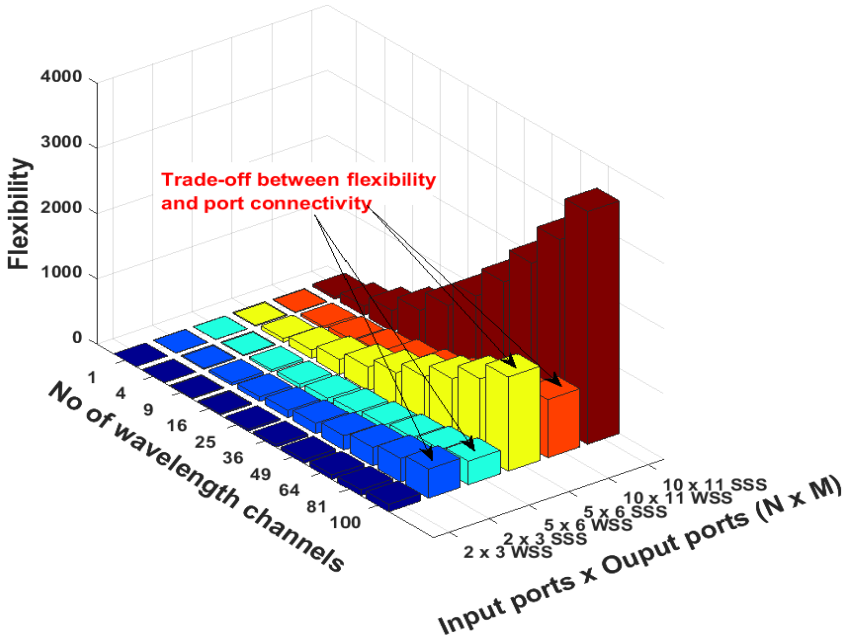

Fig. 9. Comparison of SSS and WSS across different port dimensions.

To the best of our knowledge, the maximum port dimension of a commercially available WSS is 1 × 35 WSS [45]. Fig. 10 demonstrates the measured flexibility of a WSS and SSS with a 1 × 35 port dimension. The flexibility of SSS was calculated with spectral granularity of 12.5GHz. It can be observed in Fig.10 that the SSS demonstrates 300% higher flexibility than the WSS at a spectral range of 100 wavelength channels with 50GHz channel spacing.

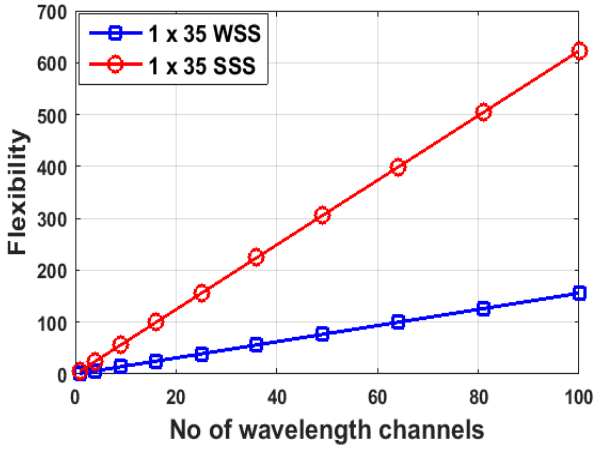

Fig. 10. Comparison of 1 × 35 WSS/SSS.

2) *N* x *M SSS with internal contention*: The *N* × *M* SSS design with internal contention is modeled the same way as the WSS design with internal wavelength contention but with a finer spectral granularity factor *k*. Therefore the flexibility of this *N* × *M* SSS design is

$$F(S) = kW log\left(\sum_{a=0}^{1} \frac{M!}{(M-a)!}\binom{N}{N-a}\right) \quad (5)$$

3) *N × M SSS with I/O port dimension reconfigurability*: This *N × M* SSS design provides I/O port dimension reconfigurability in addition to finer spectrum switching granularity. The model for measuring the flexibility of the *N × M* SSS design with port reconfigurability is modeled in a similar way to the WSS design with port reconfigurability. Thus assuming this design is contentionless, the flexibility is

$$F(S) = log\left(\sum_{N=1,}^{(P-1)} \left(\left(\sum_{a=0}^{x} \frac{(P-N)!}{((P-N)-a)!}\binom{N}{N-a}\right)^{kW}\right)\right) \quad (6)$$
$$if\ N \leq P-N, x = N\ and\ if\ N > P-N, x = P-N$$

From the theoretical analysis and results presented in this section, we note some important parameters to be considered for WSS/SSS design which include; switching dimensions (space, frequency), spectral range, port configuration, I/O port dimension reconfigurability, contention and spectral granularity. The combination and variation of these parameters offer different degrees of flexibility and performance. Therefore a WSS can be designed based on functionality or performance required without overprovision of resources. As demonstrated in Fig 3, flexibility and connectivity increase with higher port cross-connection and spectral range. Therefore if an *N × M* WSS with high connectivity and flexibility is required, the important design factors to be considered are the degree of port cross-connection (port dimension) and wavelength contention. High port cross-connection increases port connectivity as different paths for network traffic flow can be established. Secondly, an *N × M* WSS without contention improves connectivity as the selection of wavelength resources for a given traffic flow are not restricted and wavelength blocking is reduced (as demonstrated in Fig. 5). Another important design parameter critical for a WSS/SSS design with different levels of connectivity is port dimension reconfigurability. Fig. 7 shows different steps of port connectivity granularity with the corresponding degrees of flexibility. The flexibility and the level of connectivity are important for efficiently managing varying and unpredictable bidirectional traffic flows. Furthermore, such analysis mentioned above can be of assistance to network operators in different design scenarios. For instance, if an operator requires an *N × M* WSS/SSS design with flexible and scalable capacity or with node degree expansion while other KPIs are negligible. In the scenario with flexible and scalable capacity, spectral range and spectral granularity are important design parameters to be considered. This is because the switching component should be able to provide spectrum switching flexibility in terms of channel spacing to support higher traffic and modulation formats. For node degree scalability, the port dimension of the device is important, this is because there must be enough input/output ports to provision for increase in traffic demand or node expansion e.g. adding more node degrees to an existing mesh network or expanding the add/drop network.

5. Flexibility Measurement, Analysis and Design Rules for Bandwidth Variable Transponders

Network operators can select different transponder configurations based on different degrees of flexibility and performance required following network trends, resources i.e., fiber availability and end-user needs. These transponders can have a range of configurations equipped with different functionalities such as fixed/flexible rates, fixed/flexible grid and sliceable optical carrier. A set of them are described, measured and analyzed below while having their features summarized in Table 2. Note that the flexibility models presented in this section can be used to measure the flexibility of different transponder configurations from fixed to bandwidth variable and sliceable transponders.

TABLE 2
SUMMARY OF DESIGN PARAMETERS OPTIONS FOR DIFFERENT TRANSMITTER CONFIGURATIONS

Network Grid Design	Laser Type	Optical carrier Category	Programmable Features	Performance
Fixed Grid	Non –tunable	Single-carrier	Modulation format	Fixed capacity
Flexible Grid	Tunable	Multi-carrier	Symbol rate	Flexible channels
			Wavelength channels	Flexible bitrates
			Spectral slots	Flexible grid on different center frequencies
			Optical carriers	Bitrate granularity
			Electrical carriers	Super channels
				Multiple optical flows(sliceable)

5.1 Fixed Grid Bandwidth variable and sliceable transponder

In this configuration, a multi-carrier optical transmitter design with multiple bitrates in a fixed grid network is considered. Fig. 11 presents a schematic of a sliceable, tunable, bandwidth variable yet fixed grid transmitter. The transmitter consists of multiple tunable lasers, modulators and DACs each supporting one optical carrier. Assuming that the transmitter supports D optical carriers, u is the number of optical carriers that are transmitted at the same time and $(D-u)$ is the number of optical carriers that are turned off (not in use). We assume each optical carrier can be independently reconfigured to B modulations, E symbol rates and W tunable wavelength channels (assuming each carrier has the same number of programmable parameters). Additionally, we assume s number of electrical subcarriers can be generated electrically and independently configured to B modulations formats, E symbol rates and injected onto any W wavelength channels (assuming each electrical sub carrier has the same number of programmable parameters). This implies that different combinations of optical carriers with or without electrical carriers can be generated and combined to form a super channel or multiple flows of optical paths of different bandwidths. This is

achieved by turning on and turning off carriers to form optical flows based on demand which can be transmitted or sliced to a single or multiple destinations i.e., the transponder is sliceable. The flexibility of the transponder is

$$F(S) = log\left(\sum_{u=0}^{D}\left(\left(\sum_{s=1}^{S}(BE)^{s}W\right)^{u}\binom{D}{D-u}\right)\right) \qquad (7)$$

It should be noted that the flexibility model for this transmitter design were derived without considering wavelength contention between optical carriers. Furthermore the models can be used to measure the flexibility of a transponder with different configurations. For instance if the transponder designed has fixed modulation format $B = 1$ or a non-tunable laser $W = 1$. Also when the transponder has no electrical subcarrier s is 1.

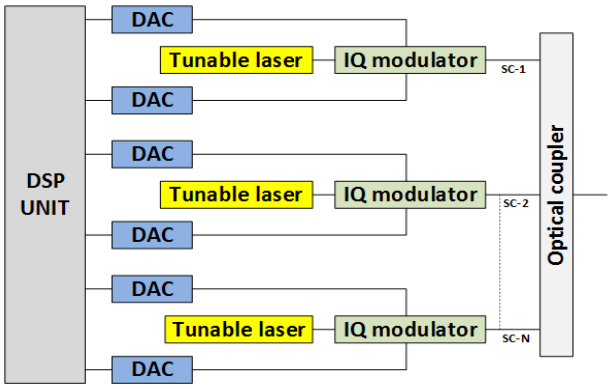

Fig. 11. Schematic of a multi-carrier transmitter.

Fig. 12 illustrates the comparison of measured flexibility using the model in Eq. (7) by varying the number of reconfigurable optical carriers and number of reconfigurable modulation formats while other parameters are kept constant. It is noted that increasing the number of optical carriers has a greater impact on flexibility than increasing the number of modulation formats. This is due to the fact that having more optical carriers provides more flexibility and connectivity in the transmitter output. Such trade-offs and analysis are important for transmitter design based on the transmission requirement.

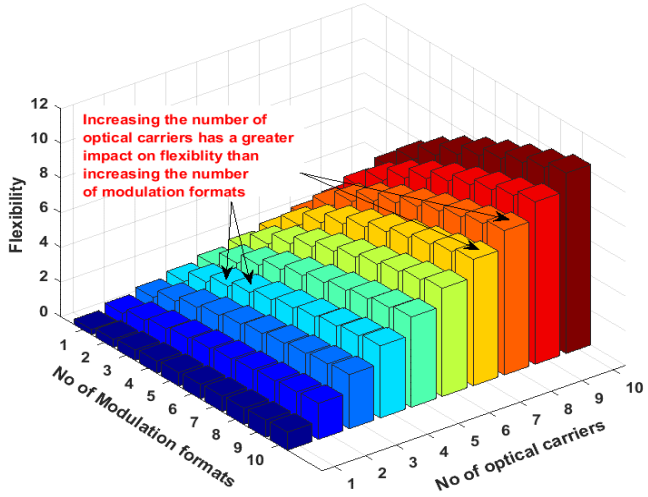

Fig. 12. Comparison of optical carriers and modulation format.

We propose a new model to consider contention between optical carriers. To achieve this we calculate the different number of combinations that tunable wavelength channels W can be selected without repetition which is $\frac{W!}{(W-u)!}$, thus the flexibility is given by

$$F(S) = log\left(\sum_{u=0}^{D}\left(\left(\sum_{s=1}^{S}(BE)^{s}\right)^{u}\frac{W!}{(W-u)!}\binom{D}{D-u}\right)\right) \qquad (8)$$

However it should be noted that this model can only be applied when the number of tunable wavelength channels W is equal or greater than the number of optical carriers D ($W \geq D$).

5.2 Flexible Grid Bandwidth variable and sliceable transponder

In this transmitter design, the tunable lasers are upgraded to flexible grid tunable lasers with finer spectral tuning granularity to support flexible grid networks. Modeled in a similar way to fixed grid bandwidth variable and sliceable transponder described above. Assuming the spectral granularity factor of the laser is equal to k. The flexibility is

$$F(S) = log\left(\sum_{u=0}^{D}\left(\left(\sum_{s=1}^{s}(BE)^{s}\, kW\right)^{u}\binom{D}{D-u}\right)\right) \quad (9)$$

Similarly for the flexibility model for this transmitter design without contention is

$$F(S) = log\left(\sum_{u=0}^{D}\left(\left(\sum_{s=1}^{s}(BE)^{s}\right)^{u}\frac{kW!}{(kW-u)!}\binom{D}{D-u}\right)\right) \quad (10)$$

However it should be stated that this model can only be applied when the number of tunable spectral slot kW is equal or greater than the number of optical carriers D ($kW \geq D$).

5.3 Design Rules and Trade-off of Flexibility of BVTs and other Figures of Merit

In order to create key design rules for BVT design, the design dependency and trade-offs of the different transmitter features and KPIs are analyzed. A comparison of the design parameters of different BVTs modules to deliver rates between 100 Gb/s and 1 Tb/s are presented in Table 3. Fig. 13(a)-(e) presents a visualization of the possible states and design transmitters features of the individual BVT modules listed in Table 3. Each plot demonstrates the trade-offs in modulations formats, line rates and lightpath reach as a result of different adaptive transmitter features. Fig. 13(f) illustrates a comparison of KPIs including; flexibility, normalized cost, maximum capacity, maximum spectral efficiency, lightpath reach, through loss and connectivity of the various BVT modules presented in Table 3.

TABLE 3
TRANSMITTER CONFIGURATIONS

Module name	Normalized cost	Feasible line rates(Gb/s)	No of Subcarriers	Baud rate per carrier	Occupied total bandwidth (GHz)	Reach (km)	Line Rate (Gb/s)	Modulation formats
CG-400-1L	9	400, 300, 200, 100	1	32	37.5	38	400	DP-256 QAM
						116	300	DP-64QAM
						536	200	DP-16QAM
						2714	100	DP-QPSK
CG-400-2L	11.7	400, 200, 100	2	32	75	536	400	DP-16QAM
						2714	200	DP-QPSK
						5429	100	DP-BPSK
CG-1T-5L	16.2	1000,500,250	5	32	175	536	1000	DP-16QAM
						2714	500	DP-QPSK
						5429	250	DP-BPSK
CG-1T-4L	18.75	1000,500,250	4	40	175	429	1000	DP-16QAM
						2171	500	DP-QPSK
						4343	250	DP-BPSK
CG-1T-3L	15	1000, 666.7, 333.3, 166.7	3	36	125	104	1000	DP-64QAM
						482	666.7	DP-16QAM
						2443	333.3	DP-QPSK
						4886	166.7	DP-BPSK

The connectivity is equivalent to the number of optical carriers that can be sliced and routed to different destinations. The spectral efficiency was calculated with 50GHz channels spacing. The through loss is calculated with Eq. (11), where L is equal to the total number of optical lasers connected to the optical coupler.

$$Through\ loss = -10log_{10}(1/L) \quad (11)$$

TABLE 4
COST SCALING

No of lasers	Reference (%)	Baud rate	Reference (%)
1	100	32.0	100
2	130	35.6	111
3	150	40	125
4	167	42.7	133
5	180		

The normalized cost is scaled with respect to the number of lasers and symbol rate as illustrated in Table 4. The cost of the CG-400-1L BVT module is used as reference with a normalized cost value of 9. T is equal to the percentage rise in cost of the number of lasers and R is equal to the percentage rise in the cost of the baud rate. Hence the equation for calculation the normalized cost is

$$Normalized\ cost = \big((T - 100\%) \times 9 + (R - 100\%) \times 9\big) + 9 \qquad (12)$$

CG-400G-1L: This BVT module is the least expensive module, it provides the lowest connectivity and flexibility when compared to the other BVT modules. This is due to the fact that this module consists of only one laser and therefore can only transmit one optical channel to a single destination at a particular time. However, the drawback of a single optical carrier comes at positive trade-off of the BVT exhibiting no through loss. Other design trade-offs of KPIs noted are in maximum capacity, spectral efficiency and lightpath reach when compared to CG-400G-2L. The CG-400-1L has an equal maximum capacity to CG-400L-2L but at a higher spectral efficiency and a lower lightpath reach. This is due the fact that the CG-400-1L BVT has the highest spectral efficient programmable modulation format of 256QAM among all the BVT modules.

CG-400L-2L: This BVT module is the second least expensive module, it also provides the second lowest flexibility and connectivity. Its low cost, flexibility and connectivity is attributed to the fact that it has only two lasers. This module has the same equivalent line rates to the CG-400-1L but offers greater flexibility and a higher connectivity because it has more programmable optical carriers. However this comes at a trade-off of a higher through loss. As discussed in section 2, the number of optical carriers has a greater impact on flexibility than the number of programmable modulation formats. Such a trade-off is demonstrated between CG-400L-1L and CG-400-2L. CG-400G-2L has a higher number of optical carriers than CG-400G-1L but has a lower number of programmable modulation format. In terms of spectral efficiency, this module has the lowest maximum spectral efficiency among all BVT modules.

CG-1T-5L: This module has highest flexibility and connectivity which is attributed to the fact that the BVT has the highest number of lasers. Therefore it is the most flexible in terms of transmitter output and has the highest number of multi-flow combination. However the merit in performance introduces a demerit of this module demonstrating the highest through loss. The CG-1T-5L has equivalent feasible line rates and maximum spectral efficiency to CG-1T-4L.

CG-1T-4L: This module is the most expensive module and this is due to the fact that it consists of 4 lasers and has a higher baud rate compared to all the other modules. This module demonstrates that the number of optical carriers as well as the DSP and electronics are important factors that determine the cost of a BVT module. This module has a higher flexibility and connectivity than CT-1T-3L and an equivalent maximum capacity.

CG-1T-3L: This module ranks in the middle in terms of flexibility, cost and connectivity. The CG-1T-3L has a maximum capacity equivalent to CG-1T-5L and CG-1T-4L but demonstrates the highest maximum spectral efficiency. However, the merit in spectral efficiency introduces a drawback of a lower lightpath reach due to the BVT design having a higher spectral efficient modulation format which is DP-64QAM.

Based on the theoretical analysis and results of different transponder modules presented above, we highlight important design parameters and study the relationship between KPIs presented in Fig. 13(f). We observe that connectivity scales directly with flexibility i.e., as the number of lasers increases the carrier connectivity increases and in turn the flexibility increases. This proportional relationship also exists between connectivity and through-loss. It is also observed that the higher the number of lasers present in the BVT module, the higher the port count of the coupler and the higher the through loss. Thus as connectivity increases so does the through loss. Furthermore, connectivity and flexibility relates directly with cost for CG-1T-1L, CG-1T-2L and CG-1T-3 L only. However the CG-1T-5L offers a higher flexibility and connectivity than CG-1T-4L but at a lower cost, this is because the CG-1T-5L has a lower baud rate electronic design. Others KPIs such as lightpath reach, capacity and spectral efficiency show no direct correlation. However design trade-offs are noted when a certain performance or a combination of KPIs are required. For instance, if an operator requires a BVT module with a high line rate of 1 Tb/s. From Fig. 13(f), we observe that three BVT modules CG-1T-3L, CG-1T-4L and CG-1T-5L offer this performance requirement with different design features. It now depends on the trade-off or other KPIs which are important to the operator. If 1Tb/s is required with a high level of flexibility and connectivity while other KPIs are negligible, the CG-1T-5L fits this profile. If cost, through loss and spectral efficiency are important factors to deliver 1Tb/s, the CG-1T-3L fits this design requirement because it has the lowest cost, lowest through loss and the highest spectral efficiency at a demerit of lower lightpath reach. Alternatively, if an operator requires a BVT design with high spectral efficiency while other indicators are negligible, the CG-400G-1L fits the profile of this performance requirement and this is because it has the most spectral efficient modulation format. Such analysis described above helps understand the relationship between KPIs and design parameters for design and deployment of BVTs for optical networks. In addition, a network operator can select different transmitter parameters with associated performance as demonstrated in Table 2.

For instance, if a single carrier transmitter with the flexible rate in a fixed grid network is required. This transmitter configuration will require a single fixed grid non-tunable laser and an electronic design with programmable modulation formats or programmable symbol rate or a combination of both depending on the performance required (e.g. variable spectral occupancy and spectral efficiency).

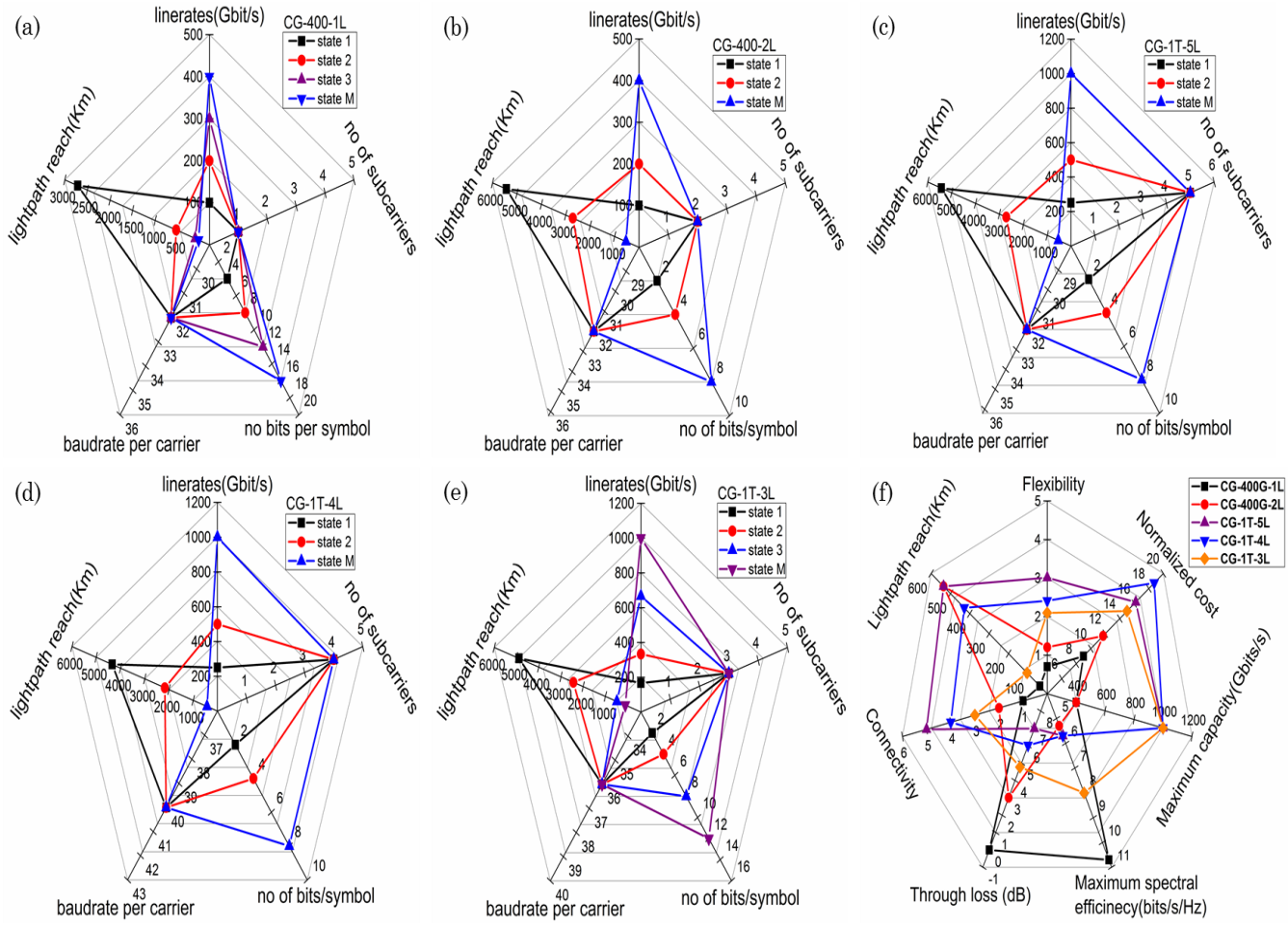

Fig. 13(a)-(e) Design parameters of the various transponder molules in table 3.
Fig. 13(f) Comparison of key performance indicators of the various transponders modules in table 3.

6. FLEXIBILITY MEASUREMENT OF KEY SUBSYSTEMS FOR ADD/DROP NETWORK DESIGN AND EONS

In this section, flexibility models of BVT subsystems for add/drop networks and EONs are proposed. Also the flexibility of these subsystems are evaluated by varying the design parameters.

Optical subsystems can be designed by the combination of different optical components with different levels of flexibility. The resultant flexibility and performance of the subsystem depends of the configuration and design of optical components used to implement the subsystem. According to [8], if a subsystem consists of two components, a with flexibility F_a and b with flexibility F_b. The resultant flexibility $F_{(a,b)}$ of the subsystem is

$$F_{(a,b)} \leq F_a + F_b \qquad (13)$$

Eq. (13) implies that the resultant flexibility $F_{(a,b)}$ of the subsystem is only equal to the sum of the individual flexibilities of components F_a and F_b if the optical components of the subsystem are disjoint.

6.1 N BVT + $N \times M$ WSS

The BVTs only offers channel flexibility not switching flexibility. Nevertheless, with a combination of the $N \times M$ WSS to form a subsystem, spectrum and space switching flexibility is achieved in addition to channel flexibility. As depicted in Fig. 14(a), each BVT is a flexible multi-carrier transmitter with programmable features for fixed grid networks. Thus a single or multiple flows optical channels of different bandwidth can be switched or blocked or independently sliced to different locations i.e., different output ports of the WSS depending on the application or

transmission requirement. This subsystem design has application in data centers networks and also provides CDC functions for ROADM design as single component provided the transponders are tunable and the WSS design is without internal wavelength contention. To obtain the flexibility we consider the subsystem as a single component. Assuming N is the number of BVTs, c is the number of BVTs transmitting at a time and therefore c is the number of active input ports on the WSS. $(N-c)$ is the number of BVTs that are off and therefore $(N-c)$ is equal to the number of input ports of the WSS that are not active. For example if c is equal to one it implies that one BVT is transmitting and one of the N input ports of the WSS is active. It is assumed that the tunable lasers in the N number of BVTs are synchronized i.e., if more than one transponder is transmitting, the same number of carriers and tunable wavelength channels are transmitted at the same time. For each BVT, we assume that D is equal to the number of optical carries, u is equal to the number of optical carriers that are transmitted at a time, $(D-u)$ is equal to the number of optical carriers that are off, s is equal to the number of programmable electrical subcarriers, B is equal to the number of programmable modulation formats, E is equal to the number of programmable symbol rates and W is equal to number of tunable wavelength channels. For the $N \times M$ WSS without contention, a is equal to the number of same wavelength channels that can be successfully passed at a time, $(c-a)$ is equal to the number of same wavelength channels that are blocked and x is the maximum number of a single wavelength that can be passed at the same time. Thus the flexibility of the subsystem is

$$F(S) = log\left(\sum_{c=1}^{N}\left(\sum_{u=1}^{D}\left(\left(\sum_{s=1}^{S}(BE)^{s}\right)^{c}\right)^{u}\frac{W!}{(W-u)!}\binom{D}{D-u} \times \left(\sum_{a=0}^{x}\frac{M!}{(M-a)!}\binom{c}{c-a}\right)^{u}\binom{N}{N-c}\right)+1\right) \quad (14)$$
$$W \geq D \; and \; if \; c \leq N \; x = c, else \; x = M$$

This model can be used to measure any configuration of the N BVT + $N \times M$ WSS.

6.2 N BVT + $N \times M$ Multicast switch

Fig. 14(b) illustrates the N BVT + $N \times M$ MCS subsystem design. Each BVT is a flexible multi-carrier transmitter and therefore provides channel flexibility for fixed grid networks. Since the multicast switch does not support filtering functions, this subsystem provides only space switching and channel flexibility. Thus super channels or multiple channel flows from the BVT can only be switched to one output port and cannot be sliced across different output ports therefore providing low connectivity. This subsystem designs is vital for implementation of ROADMs with CDC attributes. The flexibility of this subsystem is modeled in a similar way to the N BVT + $N \times M$ WSS but without spectrum switching flexibility. We assume the definition of parameters for the BVT is the same as the parameters of the BVT described in the N BVT + $N \times M$ WSS subsystem. However for the MCS, c indicates the number of input ports that are active, i indicates the number of active input ports are unblocked i.e., allow optical channels to pass at a time, and $(c-i)$ is equal to the number of active input ports that are blocked. Thus flexibility of the subsystem is

$$F(S) = log\left(\sum_{c=1}^{N}\left(\sum_{u=1}^{D}\left(\left(\sum_{s=1}^{S}(BE)^{s}\right)^{c}\right)^{u}\frac{W!}{(W-u)!}\binom{D}{D-u} \times \left(\sum_{i=0}^{x}\frac{M!}{(M-i)!}\binom{c}{c-i}\right)\binom{N}{N-c}\right)+1\right) \quad (15)$$
$$W \geq D \; and \; if \; c \leq N \; x = c, else \; x = M$$

6.3 N BVT + N × M SSS

Fig. 14(c) presents schematic of the N BVT + $N \times M$ SSS. The BVTs are flexible multi-carrier transmitters with upgraded tunable lasers with finer tuning spectral granularity for flexible grid networks. This subsystems provides channel flexibility, space switching flexibility and spectrum switching flexibility with a finer spectral granularity when compared to the N BVT + $N \times M$ WSS subsystem. This subsystem design is vital for EONs transmission requirements and realization of CDC flexible grid ROADM. The flexibility of this subsystem is derived in a similar way to the N BVT + $N \times M$ WSS subsystem but considering finer spectral granularity of the BVTs and SSS. Assuming the spectral granularity factor is k, the flexibility of the subsystem is given by

$$F(S) = log\left(\sum_{c=1}^{N}\left(\sum_{u=1}^{D}\left(\left(\sum_{s=1}^{S}(BE)^{s}\right)^{c}\right)^{u}\frac{kW!}{(kW-u)!}\binom{D}{D-u} \times \left(\sum_{a=0}^{x}\frac{M!}{(M-a)!}\binom{c}{c-a}\right)^{u}\binom{N}{N-c}\right)+1\right) \quad (16)$$
$$kW \geq D \; and \; if \; c \leq N \; x = c, else \; x = M$$

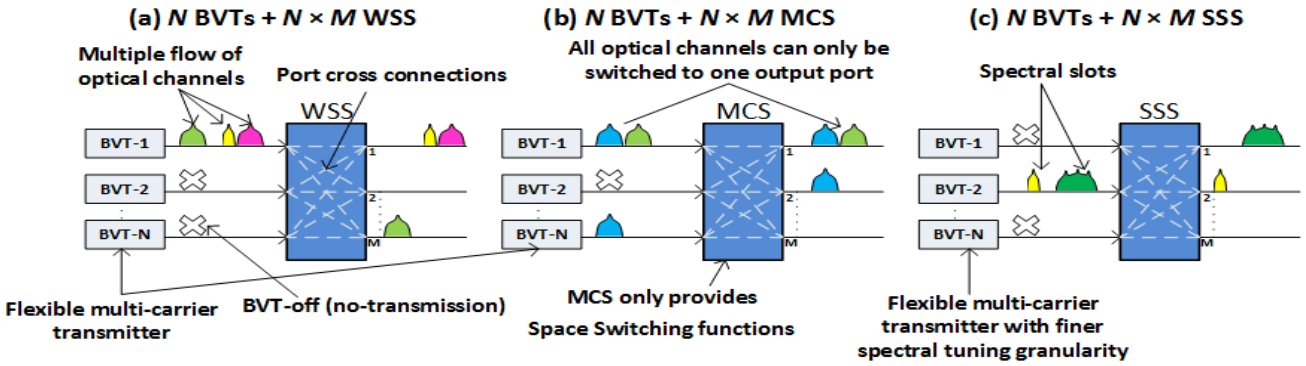

Fig. 14. Different subsystem with BVT designs.

6.4 Flexibility Analysis and Design trade-off of Subsystems

Fig. 15 illustrates the measured flexibility between the different subsystems under the same design configuration. The flexibility is measured by varying the different number of optical carriers (transmitted optical channels) while other parameters are kept constant *(B=5, E=5 and W=30)*. From Fig. 15, it is noted that increasing the number of optical carriers impact the flexibility of the 4 BVT + 4 × 16 WSS more than the 4 BVT + 4 × 16 MCS and this is attributed to the fact that the 4 BVT + 4 × 16 WSS provides space and spectrum switching functions i.e., slicing of optical channels across different output ports while the 4 BVT + 4 × 16 MCS only provides space switching functions. Increasing the optical carriers has the greatest impact on the 4 BVT + 4 × 16 SSS due to finer spectral granularity of the SSS and BVTs. Fig. 16 shows the measured flexibility between the different subsystems of the same configuration across different modulations while other parameters are kept constant (*E=5, D=10 and W=30*). It is observed that there is a general increase in the flexibility of all the subsystems. In particular, by increasing the modulation format, the flexibility has a constant impact on all subsystems as the difference in flexibility between the subsystems remain constant as the number of modulation formats increases. It is also noted in Fig. 16, that the pace of increase in flexibility reduces as the number of programmable modulation formats increases.

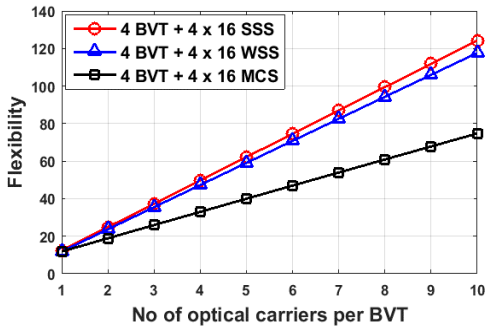

Fig. 15. Comparison of the flexibility of 4 × 16 WSS/MSC/SSS.

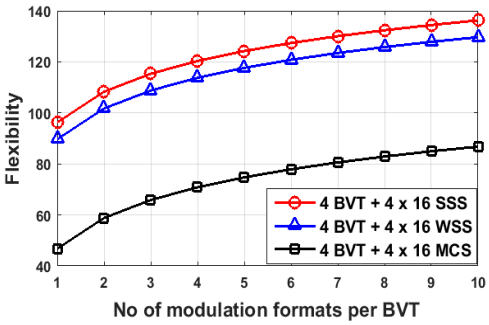

Fig. 16. Comparison of the flexibility of 4 × 16 WSS/MSC/SSS.

Based on this analysis, increasing programmable parameters of the BVT such as number of optical carriers and modulation format increases the overall flexibility of all the subsystem. However for all subsystems described, increasing the number of optical carriers has a greater impact on the pace of increase in flexibility than increasing the number of programmable modulation format. Furthermore, the design or selection of

the different subsystem will depend on the required performance or transmission requirement. For instance, a scenario where a subsystem with port connectivity, flexible channels, flexible rate and low optical carrier connectivity is required. For this scenario, the BVT design should contain tunable fixed grid lasers and programmable transmitter features. For the switching component, since optical carrier connectivity is negligible, an acceptable port configuration of MCS which supports only space switching functions maybe used to build the subsystem as slicing of optical carriers to different destinations is not required.

7. CONCLUSION

We reviewed key enabling technologies for ROADMs, add/drop networks and EONs. More importantly, we derived and proposed models to measure the flexibility of WSSs, SSSs and BVTs under different design conditions considering the component's functionalities and design parameters. We highlighted design rules for the optical components using design dependency and trade-off of KPIs and variable parameters based on theoretical analysis and results presented. Additionally, independent optical components were combined to form complete BVT subsystem. Based on this analysis, models to measure the flexibility of these subsystems were derived and proposed. The flexibility and design trade-off of these subsystems were analyzed. Finally, the approach of designing optical components and subsystem such as add/drop network and bypass architectures used in ROADMs using flexibility as a figure of merit and other measurable KPIs, provides network operators and vendors rules for designing elements for a certain transmission and network performance requirement.

ACKNOWLEDGMENT

This work is supported by ESPRC grant: EP/L0207070/1 SONATAS. The authors also appreciate Simon Poole from Finisar, Australia for his contributions to discussions on the analysis of this paper.

REFERENCES

[1] "Cisco Visual Networking Index: Forecast and Methodology, 2013-2018," Cisco white paper (online). Available at http://www.cisco.com/c/en/us/solutions/collateral/service-provider/ip-ngn-ip-next-generation-network/white_paper_c11-481360.html.

[2] O. Gerstel, M. Jinno, A. Lord and S. J. B. Yoo, "Elastic optical networking: a new dawn for the optical layer" *IEEE Communications Magazine*, vol. 50, no. 2, pp. s12-s20, 2012.

[3] A. Napoli, M. Bohn, D. Rafique, A. Stavdas, N. Sambo, L. Poti, M. Nölle, J. K. Fischer, E. Riccardi, A. Pagano, A. Di Giglio, M. S. Moreolo, J. M. Fabrega, E. Hugues-Salas, G. Zervas, D. Simeonidou, P. Layec, A. D'Errico, T. Rahman and J. P. F. P. Giménez , "Next generation elastic optical networks: The vision of the European research project IDEALIST," *IEEE Communications Magazine*, vol.53, no.2, pp.152-162, 2015.

[4] O. Rival and A. Morea, "Cost-efficiency of mixed 10-40-100Gb/s networks and elastic optical networks," in *Optical Fiber Communication Conference/National Fiber Optic Engineers Conference*, 2011, paper OTuI4.

[5] B. Kozicki, H. Takara, Y. Sone, A. Watanabe, and M. Jinno, "Distance-Adaptive Spectrum Allocation in Elastic Optical Path Network (SLICE) with Bit per Symbol Adjustment," in *Optical Fiber Communication Conference* 2010, paper OMU3.

[6] A. Morea, A. Fen Chong and O. Rival, "Impact of transparent network constraints on capacity gain of elastic channel spacing," in *Optical Fiber Communication Conference/National Fiber Optic Engineers Conference*, 2011, paper JWA062

[7] J. L. Vizcaino, Y. Ye and I. T. Monroy, "Energy efficiency in elastic-bandwidth optical networks," in *International Conference on the Network of the Future*, 2011, pp.107-111.

[8] N. Amaya, G. Zervas, and D. Simeonidou, "Introducing node architecture flexibility for elastic optical networks," *IEEE/OSA Journal of Optical Communications and Networking*, vol. 5, no. 6, pp. 593-608, 2013.

[9] S. Gringeri, B. Basch, V. Shukla, R. Egorov, and T. J. Xia, "Flexible architectures for optical transport nodes and networks," *IEEE Communications Magazine*, vol. 48, no. 7, pp. 40-50, 2010.

[10] R. Jensen, A. Lord, and N. Parsons, "Colourless, directionless, contentionless ROADM architecture using low-loss optical matrix switches," in *European Conference and Exhibition Optical Communication*, 2010, pp.1-3

[11] K. Takaha, Y. Mori, H. Hasegawa, K. Sato and T. Watanabe, "A 204.8 Tbps Throughput 64x64 Optical Cross-Connect Prototype that Allows C/D/C Add/Drop," in *Optical Fiber Communication Conference*, 2014, paper M2K.1.

[12] W. I. Way, "Optimum Architecture for M×N Multicast Switch-Based Colorless, Directionless, Contentionless, and Flexible-Grid ROADM," in *Optical Fiber Communication Conference/National Fiber Optic Engineers Conference*, 2012, paper NW3F.5

[13] R. Jensen, "Optical Switch Architectures for Emerging Colorless/Directionless/Contentionless ROADM Networks," in *Optical Fiber Communication Conference/National Fiber Optic Engineers Conference*, 2011, paper OThR3.

[14] Y. Sakamaki, T. Kawai, T. Komukai, M. Fukutoku, T. Kataoka, T. Watanabe and Y. Ishii, "Experimental demonstration of colourless, directionless, contentionless ROADM using 1×43 WSS and PLC-based transponder aggregator for 127-Gbit/s DP-QPSK system," in *European Conference on Optical Communication*, 2011, pp 1-3

[15] A. Peters, E. Hugues-Salas, G. Zervas and D. E. Simeonidou, "Measuring Flexibility and Design Trade-offs of N x M SSS-based ROADMs and BVTs," in *Optical Fiber Communication Conference*, 2015, paper W3J.5.

[16] A. Peters, E. Hugues-Salas, G. Zervas and D. E. Simeonidou, "Design of Elastic Optical Nodes based on Subsystem Flexibility Measurement and other Figures of Merit," in *European Conference on Optical Communication*, 2015, pp.1-3

[17] B. Collings, "Physical layer components, architectures and trends for agile photonic layer mesh networking," in *European Conference on Optical Communication*, 2009. pp.1-3

[18] "A performance comparison of WSS switch Engine Technologies," JDSU whitepaper (online). Available at http://www.jdsu.com/productliterature/wsscomp_wp_cms_ae.pdf

[19] G. Baxter, S. Frisken, D. Abakoumov, H. Zhou, I. Clarke, A. Bartos and S. Poole, "Highly Programmable Wavelength Selective Switch Based on Liquid Crystal on Silicon Switching Elements," in *Optical Fiber Communication Conference and Exposition and The National Fiber Optic Engineers Conference*, 2006, paper OTuF2.

[20] D. M. Marom, D. T. Neilson, D. S. Greywall, P. Chien-Shing, N. R. Basavanhally, V. A. Aksyuk, D. O. Lopez, F. Pardo, M. E. Simon, Y. Low, P. Kolodner and C. A. Bolle, "Wavelength-selective 1×K switches using free-space optics and MEMS micromirrors: theory, design, and implementation," *Journal of Lightwave Technology*, vol.23, no.4, pp.1620-1630, 2005.

[21] N. K. Fontaine, R. Ryf, and D. T. Neilson, "N×M Wavelength Selective Crossconnect with Flexible Passbands," in *Optical Fiber Communication Conference*, 2012, paper PDP5B.2.

[22] F. Xiao and K. Alameh, "Opto-VLSI-based N × M wavelength selective switch," Optics Express, vol.21, no.15, pp.18160–18169, 2013

[23] T. Zami and B. Lavigne, "Benefit of pure NxM WSS for optical multiflow application," in *Optical Fiber Communication Conference/National Fiber Optic Engineers Conference*, 2013, paper OTh4B.2.

[24] International Telecommunication Union. G.694.1: Spectral grids for WDM applications: DWDM frequency grid (online). Available at: http://www.itu.int/rec/T-REC-G.694.1-201202-I/en

[25] M. Jinno, H. Takara, B. Kozicki, Y. Tsukishima, Y. Sone and S. Matsuoka, "Spectrum-efficient and scalable elastic optical path network: architecture, benefits, and enabling technologies," *IEEE Communications Magazine*, vol.47, no.11, pp.66-73, 2009.

[26] E. Hugues-Salas, G. Zervas, D. Simeonidou, E. Kosmatos, T. Orphanoudakis, A. Stavdas, M. Bohn, A. Napoli, T. Rahman, F. Cugini, N. Sambo, S. Frigerio, A. D'Errico, A. Pagano, E. Riccardi, V. Lopez and J.P.F.P Gimenez, "Next generation optical nodes: The vision of the European research project IDEALIST," *IEEE Communications Magazine*, vol.53, no.2, pp.172,181, 2015

[27] T. Watanabe, K. Suzuki, T. Goh, K. Hattori, A. Mori, T. Takahashi, T. Sakamoto, K. Morita, S. Sohma and S. Kamei, "Compact PLC-based Transponder Aggregator for Colorless and Directionless ROADM," in *Optical Fiber Communication Conference/National Fiber Optic Engineers Conference*, 2011, paper OTuD3.

[28] T. Watanabe, K. Suzuki and T. Takahashi, "Silica-based PLC Transponder Aggregators for Colorless, Directionless, and Contentionless ROADM," in *Optical Fiber Communication Conference/National Fiber Optic Engineers Conference*, 2012, paper OTh3D.1.

[29] R. Schmogrow, D. Hillerkuss, M. Dreschmann, M. Huebner, M, Winter, J. Meyer, B. Nebendahl, C. Koos, J. Becker, W. Freude and J. Leuthold, "Real-Time Software-Defined Multiformat Transmitter Generating 64QAM at 28 GBd," *IEEE Photonics Technology Letters*, vol.22, no.21, pp.1601-1603, 2010.

[30] W. Freude, R. Schmogrow, B. Nebendahl, D. Hillerkuss, J. Meyer, M. Dreschmann, M. Huebner, J. Becker, C. Koos and J. Leuthold, "Software-defined optical transmission," in *International Conference on Transparent Optical Networks*, pp.1-4, 2011

[31] J. Hilt, M. Nolle, L. Molle, M. Seimetz and R. Freund, "32 Gbaud real-time FPGA-based multi-format transmitter for generation of higher-order modulation formats," in *International Conference on Optical Internet*, 2010, pp.1-3,

[32] W. Shieh, H. Bao and Y. Tang, "Coherent optical OFDM: theory and design," *Optics Expres*s, vol.16, pp. 841–59, 2008.

[33] Y. Zhang, M. O'Sullivan and R. Hui, "Digital subcarrier multiplexing for flexible spectral allocation in optical transport network," *Optics Express*, Vol 19, pp. 21880-21889, 2011.

[34] A. Sano, E. Yamada, H. Masuda, E. Yamazaki, T. Kobayashi, E. Yoshida, Y. Miyamoto, R. Kudo, K. Ishihara and Y. Takatori, "No-Guard-Interval Coherent Optical OFDM for 100-Gb/s Long-Haul WDM Transmission," *Journal of Lightwave Technology*, vol.27, pp. 3705-3713, 2009.

[35] G. Bosco, V. Curri, A. Carena, P. Poggiolini and F. Forghieri, "On the Performance of Nyquist-WDM Terabit Superchannels Based on PM-BPSK, PM-QPSK, PM-8QAM or PM-16QAM Subcarriers," *Journal of Lightwave Technology*, vol.29, no.1, pp.53-61, 2011.

[36] D. J. Geisler, N. K. Fontaine, R. P. Scott, T. He, L. Paraschis, O. Gerstel, J. P. Heritage and S. J. B. Yoo, "Bandwidth scalable, coherent transmitter based on the parallel synthesis of multiple spectral slices using optical arbitrary waveform generation," *Optics Express*, vol.19, pp.8242-8253, 2011.

[37] M. Jinno, H. Takara, Y. Sone, K. Yonenaga and A. Hirano, "Multiflow optical transponder for efficient multilayer optical networking," *IEEE Communications Magazine*, vol.50, no.5, pp.56-65, 2012.

[38] N. Sambo, A. D'Errico, C. Porzi, V. Vercesi, M. Imran, F. Cugini, A. Bogoni, L. Potì, and P. Castoldi, "Sliceable transponder architecture including multiwavelength source," *IEEE/OSA Journal of Optical Communications and Networking*, vol.6, no.7, pp.590-600, 2014

[39] S. Yan, Y. Yan, B.R Rofoee, Y. Shu, E. Hugues-Salas, G. Zervas, and D. Simeonidou, "Real-Time Ethernet to Software-Defined Sliceable Superchannel Transponder," *Journal of Lightwave Technology*. vol.33, no.8, pp.1571-1577, 2015.

[40] N. Sambo, P. Castoldi, A. D'Errico, E. Riccardi, A. Pagano, M.S. Moreolo, J. M. Fàbrega, D. Rafique, A. Napoli, S. Frigerio, E. H. Salas, G. Zervas, M. Nolle, J. K. Fischer, A. Lord and J. P. F. P. Giménez "Next generation sliceable bandwidth variable transponders," *IEEE Communications Magazine*, vol.53, no.2, pp.163-171, 2015.

[41] V. Lopez, B. de la Cruz, O. G. de Dios, O. Gerstel, N. Amaya, G. Zervas, D. Simeonidou and J. P. Fernandez-Palacios, "Finding the target cost for sliceable bandwidth variable transponders," , *IEEE/OSA Journal of Optical Communications and Networking*, vol.6, no.5, pp.476-485, 2014.

[42] M. Garrich Alabarce, J. Oliveira, M. Siqueira, N. Amaya, G. S. Zervas, D. E. Simeonidou and J. Oliveira, "Flexibility of Programmable Add/Drop Architecture for ROADMs," in *Optical Fiber Communication Conference*, 2014, paper W1C.2.

[43] "Finisar Wave Shaper 16000S multiport optical processor", (online). Available at https://www.finisar.com/sites/default/files/downloads/waveshaper_16000s_product_brief_11_14_0.pdf

[44] G. Saridis, E. Hugues-Salas, Y. Yan, S. Yan, S. Poole, G. Zervas, and D. Simeonidou, "DORIOS: Demonstration of an All-Optical Distributed CPU, Memory, Storage Intra DCN Interconnect," in *Optical Fiber Communication Conference*, 2015, paper W1D.2.

[45] "TrueFlex Twin 1x35 Wavelength Selective Switch (Twin 1x35 WSS)" (online). Available at https://www.lumentum.com/en/products/trueflex-twin-1x35-wavelength-selective-switch